NUWC-NPT Technical Report 11,856
24 February 2008

Response of a Beam on a Highly Elastic Foundation

Andrew J. Hull
Autonomous and Defensive Systems Department

NAVSEA
WARFARE CENTERS
NEWPORT

20080701 277

Naval Undersea Warfare Center Division
Newport, Rhode Island

PREFACE

The work described in this report was sponsored by the Office of Naval Research (ONR) under the project entitled "Validating the Structural Response of Elastomeric and 1-3 Piezoceramic Plates," ONR funding document number N0001408WX20092, program manager David Drumheller (ONR 333).

The technical reviewer for this report was John R. Welch (Code 8212).

Reviewed and Approved: 24 February 2008

James S. Griffin
Head, Autonomous and Defensive Systems Department

REPORT DOCUMENTATION PAGE

Form Approved
OMB No. 0704-0188

1. REPORT DATE (*DD-MM-YYYY*)
24 February 2008

2. REPORT TYPE
Final

3. DATES COVERED (*From – To*)

4. TITLE AND SUBTITLE
Response of a Beam on a Highly Elastic Foundation

5a. CONTRACT NUMBER

5b. GRANT NUMBER

5c. PROGRAM ELEMENT NUMBER

6. AUTHOR(S)
Andrew J. Hull

5d. PROJECT NUMBER

5e. TASK NUMBER

5f. WORK UNIT NUMBER

7. PERFORMING ORGANIZATION NAME(S) AND ADDRESS(ES)
Naval Undersea Warfare Center Division
1176 Howell Street
Newport, RI 02841-1708

8. PERFORMING ORGANIZATION REPORT NUMBER
TR 11,856

9. SPONSORING/MONITORING AGENCY NAME(S) AND ADDRESS(ES)
Office of Naval Research
875 North Randolph Street
Arlington VA 22203-1995

10. SPONSORING/MONITOR'S ACRONYM
ONR

11. SPONSORING/MONITORING REPORT NUMBER

12. DISTRIBUTION/AVAILABILITY STATEMENT
Approved for public release; distribution is unlimited.

13. SUPPLEMENTARY NOTES

14. ABSTRACT

This report develops and analyzes the equations of motion of an infinite Euler-Bernoulli beam that is in contact with a set of periodic support beams. The support beams are modeled as Euler-Bernoulli beams in their transverse directions and modeled using the wave equation in their axial directions. This new formulation allows the support beam models to admit wave propagation so that the dynamic effects of a long foundation can be understood. Three different loading cases are analyzed and the results are discussed.

15. SUBJECT TERMS
Elastic Foundation   Euler-Bernoulli Beam   Wave Equation

16. SECURITY CLASSIFICATION OF: a. REPORT	b. ABSTRACT	c. THIS PAGE	17. LIMITATION OF ABSTRACT	18. NUMBER OF PAGES	19a. NAME OF RESPONSIBLE PERSON
(U)	(U)	(U)	SAR	26	Andrew J. Hull
					19b. TELEPHONE NUMBER (*Include area code*) 401-832-5189

TABLE OF CONTENTS

LIST OF ILLUSTRATIONS

RESPONSE OF A BEAM ON A HIGHLY ELASTIC FOUNDATION

1. INTRODUCTION

The response of beams subjected to various loading conditions is an ongoing field of study.[1] Over the years, the effects of stiffeners modeled as springs has been added to the various models of strings,[2,3] beams,[4,5] shells,[6,7] and plates.[8,9,10] The modeled stiffener is typically a rib-like attachment to the structure whose thickness is small enough that the rib behavior can be approximated by a model of a discrete spring. There are structures, however, like tall bridges, where the length of the stiffener is long, and the dynamic effects cannot be accurately modeled as a discrete spring. In this report, the dynamics of a beam on an elastic foundation is formulated and analyzed. The horizontal beam is modeled as an Euler-Bernoulli beam in the transverse direction. The stiffeners are modeled as Euler-Bernoulli beams in their transverse direction and modeled using the wave equation in their axial direction so that wave propagation effects are present in the analysis. The two models are joined using appropriate boundary conditions and then the systems' corresponding displacements are calculated. Three different loading conditions are analyzed and the results are discussed.

2. SYSTEM MODEL

The system model consists of an infinite horizontal Euler-Bernoulli beam on a foundation of finite length equally-spaced vertical beams. The vertical beams are governed by the Euler-Bernoulli equation in their transverse direction and the wave equation in their axial direction. The system configuration is shown in figure 1. The model uses the following assumptions: (1) the forcing function acting on the system is at a definite frequency, (2) the motion of the horizontal beam is in the transverse direction, (3) the horizontal beam has infinite spatial extent in the x-direction, (4) the motion of the vertical beams is in the transverse and axial directions, (5) there is no coupling between the transverse and axial motion of the vertical beams, (6) the particle motion is linear, and (7) the horizontal beam is rigidly connected to the vertical beams.

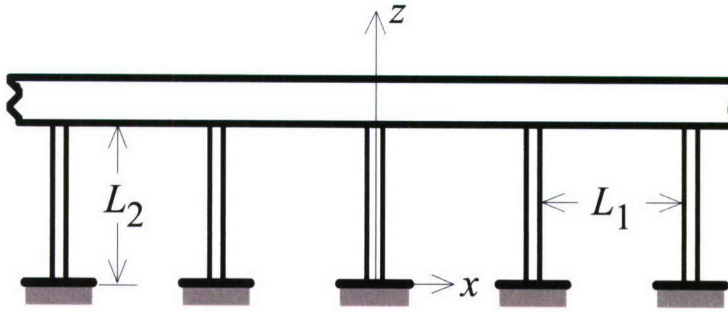

Figure 1. Beam on Elastic Foundation

The horizontal Euler-Bernoulli beam is governed by the equation

$$E_1 I_1 \frac{\partial^4 w(x,t)}{\partial x^4} + \rho_1 A_1 \frac{\partial^2 w(x,t)}{\partial t^2} + \sum_{n=-\infty}^{n=+\infty} F_n \delta(x - nL_1) + \frac{\partial}{\partial x}\left[\sum_{n=-\infty}^{n=+\infty} M_n \delta(x - nL_1)\right] = f(x,t), \quad (1)$$

where $w(x,t)$ is the transverse displacement of the horizontal beam (m), E is Young's modulus $(\mathrm{N/m^2})$, I is the moment of inertia $(\mathrm{m^4})$, ρ is density $(\mathrm{kg/m^3})$, A is the area $(\mathrm{m^2})$, F_n is the force exerted by each vertical beam (N), M_n is the moment exerted by each vertical beam (Nm), L_1 is the spacing of the vertical beams (m), δ is the Dirac delta function (1/m), x is the spatial position (m), t is time (s), $f(x,t)$ is the external forcing function per unit length acting on the beam (N/m), and the subscript 1 denotes the properties of the horizontal beam. The vertical beams are governed by the equations

$$E_2 I_2 \frac{\partial^4 u_n(z,t)}{\partial z^4} + \rho_2 A_2 \frac{\partial^2 u_n(z,t)}{\partial t^2} = 0, \quad (2)$$

and

$$E_2 \frac{\partial^2 v_n(z,t)}{\partial x^2} - \rho_2 \frac{\partial^2 v_n(z,t)}{\partial t^2} = 0, \quad (3)$$

where $u_n(x,t)$ is the transverse displacement (m) of the nth vertical beam, $v_n(x,t)$ is the axial displacement (m) of the nth vertical beam, and the subscript 2 denotes the properties of the vertical supports.

The boundary conditions on the vertical beams at the base of the structure ($z = 0$) are zero displacement in the axial direction, zero displacement in the transverse direction, and zero slope in the transverse direction. Mathematically, these are written as

$$v_n(0,t) = 0\,, \tag{4}$$

$$u_n(0,t) = 0\,, \tag{5}$$

and

$$\frac{\partial u_n(0,t)}{\partial z} = 0\,, \tag{6}$$

respectively. The first boundary condition at the interface of the horizontal and vertical beams requires that they have the same displacement in the vertical direction, and this is written as

$$v_n(L_2,t) = w(x - nL_1,t)\,. \tag{7}$$

The second boundary condition at the interface of the beams requires that the transverse displacement of the vertical beam equal zero because the horizontal beam does not have a degree of freedom in the horizontal direction, i.e.,

$$u_n(L_2,t) = 0\,, \tag{8}$$

and the third is that the slope of the horizontal beam is negative of the slope of the vertical beam because their attachment point is modeled as a rigid connection. This boundary condition is

$$\frac{\partial u_n(L_2,t)}{\partial z} = -\frac{\partial w(x - nL_1,t)}{\partial x}\,. \tag{9}$$

The above nine expressions represent a mathematical model of the system with external forcing on the horizontal beam.

3. ANALYTICAL SOLUTION

The problem is first solved for excitation of the horizontal beam. For a spatially infinite system periodic on $[0, L_1]$, the horizontal beam displacement can be written in series form equal to a sum of unknown coefficients multiplied by a spatially-indexed harmonic exponential function in the x-direction multiplied by an exponential harmonic function in time. The horizontal beam displacement becomes

$$w(x,t) = \sum_{m=-\infty}^{m=+\infty} W_m \exp(\mathrm{i}k_m x)\exp(-\mathrm{i}\omega t)\,, \tag{10}$$

where W_m are the unknown coefficients and

$$k_m = k + \frac{2\pi m}{L_1}\,, \tag{11}$$

where k is wavenumber (rad/m) and ω is frequency (rad/s). Once the analytical form of the beam displacement has been determined (equation (10)), the axial displacement of the vertical beams at some location x can be determined using equations (3), (4), and (7), which gives

$$v_n(z,t) = \frac{\sin(hz)}{\sin(hL_2)} \sum_{m=-\infty}^{m=+\infty} W_m \exp(\mathrm{i}k_m x)\exp(-\mathrm{i}\omega t)\,, \tag{12}$$

where

$$h = \omega\sqrt{\frac{\rho_2}{E_2}}\,. \tag{13}$$

Each individual force at the top end of the vertical beam is given by

$$F_n = A_2 E_2 \frac{\partial v_n(L_2,t)}{\partial z} = A_2 E_2 h \cot(hL_2) \left[\sum_{m=-\infty}^{m=+\infty} W_m \exp(\mathrm{i}k_m x) \right] \exp(-\mathrm{i}\omega t) . \tag{14}$$

The transverse displacement of the vertical beams at some location x can be determined using equations (2), (5), (6), (8), and (9), which gives

$$\begin{aligned} u(z,t) = \Bigg\{ & \frac{\cosh(\beta L_2)\sin(\beta z) + \cos(\beta L_2)\sinh(\beta z) - \sin(\beta L_2)\cosh(\beta z)}{2\beta\cos(\beta L_2)\cosh(\beta L_2)} + \\ & \frac{-\sinh(\beta L_2)\cos(\beta z) - \sin[\beta(z-L_2)] - \sinh[\beta(z-L_2)]}{2\beta\cos(\beta L_2)\cosh(\beta L_2)} \Bigg\} \\ & \frac{\partial}{\partial x} \left[\sum_{m=-\infty}^{m=+\infty} W_m \exp(\mathrm{i}k_m x) \right] \exp(-\mathrm{i}\omega t) , \end{aligned} \tag{15}$$

where

$$\beta = \left[\frac{\rho_2 A_2 \omega^2}{E_2 I_2} \right]^{1/4} . \tag{16}$$

Each individual moment at the top end of the vertical beam is given by

$$\begin{aligned} M_n &= E_2 I_2 \frac{\partial^2 v_n(L_2,t)}{\partial z^2} \\ &= \frac{E_2 I_2 \beta[\sin(\beta L_2)\cosh(\beta L_2) - \sinh(\beta L_2)\cos(\beta L_2)]}{1-\cos(\beta L_2)\cosh(\beta L_2)} \frac{\partial}{\partial x} \left[\sum_{m=-\infty}^{m=+\infty} W_m \exp(\mathrm{i}k_m x) \right] \exp(-\mathrm{i}\omega t) . \end{aligned} \tag{17}$$

Then equations of the unknown wave propagation coefficients are now determined by inserting equations (10), (14), and (17) into equation (1). Also, the assumption that the forcing function is harmonic in time allows it to be written as

$$f(x,t) = g(x)\exp(-\mathrm{i}\omega t) \tag{18}$$

and inserted into equation (1). After some manipulation and orthogonalization,[11] the m-indexed equations for the wave propagation coefficients are

$$\begin{aligned}
&\left[E_1 I_1 k_m^4 - \rho_1 A_1 \omega^2\right] W_m + \frac{A_2 E_2 h}{L_1}\cot(hL_2)\sum_{n=-\infty}^{n=+\infty} W_n \\
&+ \frac{E_2 I_2 \beta[\sin(\beta L_2)\cosh(\beta L_2) - \sinh(\beta L_2)\cos(\beta L_2)]k_m}{L_1[1-\cos(\beta L_2)\cosh(\beta L_2)]}\sum_{n=-\infty}^{n=+\infty} W_n k_n \\
&= \frac{1}{L_1}\int_0^{L_1} g(x)\exp(-\mathrm{i}k_m x)dx\,.
\end{aligned} \tag{19}$$

Equation (19) can be written as a system of equations in matrix form as

$$[\mathbf{A}]\{\mathbf{W}\} + [\mathbf{B}]\{\mathbf{W}\} + [\mathbf{C}]\{\mathbf{W}\} = \{\mathbf{D}\}\,. \tag{20}$$

where **A**, **B**, and **C** are matrices that represent the dynamics of the horizontal beam, the force of the vertical beams acting on the horizontal beam, and the moment of the vertical beams acting on the horizontal beam, respectively, **W** is the vector of unknown wave propagation coefficients, and **D** is a vector that models the excitation on the structure. The entries of equation (20) are given by

$$[\mathbf{A}] = \begin{bmatrix} \ddots & & \vdots & & ⋰ \\ & a_{-1} & 0 & 0 & \\ \cdots & 0 & a_0 & 0 & \cdots \\ & 0 & 0 & a_1 & \\ ⋰ & & \vdots & & \ddots \end{bmatrix}, \tag{21}$$

with

$$a_m = E_1 I_1 k_m^4 - \rho_1 A_1 \omega^2\,; \tag{22}$$

$$
[\mathbf{B}] = \begin{bmatrix} \ddots & & \vdots & & \iddots \\ & b & b & b & \\ \cdots & b & b & b & \cdots \\ & b & b & b & \\ \iddots & & \vdots & & \ddots \end{bmatrix}, \tag{23}
$$

with

$$
b = \frac{A_2 E_2 h}{L_1} \cot\left(h L_2\right); \tag{24}
$$

$$
[\mathbf{C}] = \begin{bmatrix} \ddots & & \vdots & & \iddots \\ & c k_{-1} k_{-1} & c k_{-1} k_0 & c k_{-1} k_1 & \\ \cdots & c k_0 k_{-1} & c k_0 k_0 & c k_0 k_1 & \cdots \\ & c k_1 k_{-1} & c k_1 k_0 & c k_1 k_1 & \\ \iddots & & \vdots & & \ddots \end{bmatrix}, \tag{25}
$$

with

$$
c = \frac{E_2 I_2 \beta [\sin(\beta L_2) \cosh(\beta L_2) - \sinh(\beta L_2) \cos(\beta L_2)]}{L_1 [1 - \cos(\beta L_2) \cosh(\beta L_2)]}; \tag{26}
$$

$$
\{\mathbf{W}\} = \begin{Bmatrix} \vdots \\ W_{-1} \\ W_0 \\ W_1 \\ \vdots \end{Bmatrix}; \tag{27}
$$

and

$$\{\mathbf{D}\} = \begin{Bmatrix} \vdots \\ \dfrac{1}{L_1}\int_0^{L_1} g(x)\exp(-\mathrm{i}k_{-1}x)dx \\ \dfrac{1}{L_1}\int_0^{L_1} g(x)\exp(-\mathrm{i}k_0 x)dx \\ \dfrac{1}{L_1}\int_0^{L_1} g(x)\exp(-\mathrm{i}k_1 x)dx \\ \vdots \end{Bmatrix}. \tag{28}$$

Three specific loading cases are examined: (1) a point load applied to the horizontal beam, (2) a moment load applied to the horizontal beam, and (3) a single axial displacement driven vertical beam. If the forcing function is an applied point load on the horizontal beam at $x = a$ with magnitude F, then

$$g(x) = F\delta(x-a), \tag{29}$$

and the load vector (equation (28)) becomes

$$\{\mathbf{D}\} = (F / L_1)\begin{Bmatrix} \vdots \\ \exp(\mathrm{i}k_{-1}a) \\ \exp(\mathrm{i}k_0 a) \\ \exp(\mathrm{i}k_1 a) \\ \vdots \end{Bmatrix}. \tag{30}$$

If the forcing function is an applied point moment on the horizontal beam at $x = a$ with magnitude M, then

$$g(x) = \frac{\partial}{\partial x}[M\delta(x-a)], \tag{31}$$

and the load vector (equation (28)) becomes

$$\{\mathbf{D}\} = \mathrm{i}(M / L_1)\begin{Bmatrix} \vdots \\ k_{-1}\exp(\mathrm{i}k_{-1}a) \\ k_0\exp(\mathrm{i}k_0 a) \\ k_1\exp(\mathrm{i}k_1 a) \\ \vdots \end{Bmatrix}. \tag{32}$$

If the forcing function is axial motion of the vertical beam at $x = 0$ with magnitude V, then equation (4) is replaced with

$$v_n(0,t) = \begin{cases} V\exp(-\mathrm{i}\omega t) & n = 0 \\ 0 & n \neq 0 \end{cases}, \tag{33}$$

then the forcing function becomes

$$g(x) = VA_2E_2h\csc(hL_2)\delta(x) \tag{34}$$

and the load vector (equation (28)) becomes

$$\{\mathbf{D}\} = (V / L_1)A_2E_2h\csc(hL_2)\begin{Bmatrix} \vdots \\ 1 \\ 1 \\ 1 \\ \vdots \end{Bmatrix}. \tag{35}$$

Once the load vector has been defined, the solution to the wave propagation coefficients can be determined by

$$\{\mathbf{W}\} = [\mathbf{A} + \mathbf{B} + \mathbf{C}]^{-1}\{\mathbf{D}\}. \tag{36}$$

The solutions in the subsequent sections will be examined in the wavenumber-frequency domain. For a function that is periodic on the interval $[0, L_1]$, the Fourier transform into the wavenumber domain is

$$\hat{w}(k,\omega) = \frac{1}{L_1}\int_0^{L_1} w(x,t)\exp(-\mathrm{i}kx)dx = W_0 \exp(-\mathrm{i}\omega t), \tag{37}$$

where the caret denotes a function in the wavenumber domain.

4. MODEL VALIDATION

The problem is first examined from a model validation standpoint. A low-frequency solution to this problem has been previously derived[12] using an energy method, and their set of indexed equations for the wave propagation coefficients are

$$\left[E_1 I_1 k_m^4 - \rho_1 A_1 \omega^2\right] W_m + \frac{K_T}{L_1}\sum_{n=-\infty}^{n=+\infty} W_n + \frac{K_R}{L_1}\sum_{n=-\infty}^{n=+\infty} W_n k_n k_m = \frac{1}{L_1}\int_0^{L_1} g(x)\exp(-\mathrm{i}k_m x)dx\,, \tag{38}$$

where K_T is the translational spring constant and K_R is the rotational spring constant. For low-frequency behavior, the following approximate expressions for the spring constants can be used:

$$K_T = \frac{A_2 E_2}{L_2} \tag{39}$$

and

$$K_R = \frac{4E_2 I_2}{L_2}\,. \tag{40}$$

If the forcing function is an applied point load on the horizontal beam at $x = a$ with magnitude F, then equations (29) and (30) define the loading vector on the right-hand side of the equation. If the forcing function is an applied point moment on the horizontal beam at $x = a$ with magnitude M, then equations (31) and (32) define the loading vector. If the forcing function is axial motion of the vertical spring at $x = 0$ with magnitude V, then the loading vector becomes

$$\{\mathbf{D}\} = (V / L_1)(A_2 E_2 / L_2)\begin{Bmatrix} \vdots \\ 1 \\ 1 \\ 1 \\ \vdots \end{Bmatrix}. \tag{41}$$

A comparative model is now assembled and analyzed at low frequency. The following parameters are used for the horizontal beam: width a_1 of 0.0508 m, thickness b_1 of 0.0254 m, moment of inertia I_1 of 6.93×10^{-11} m^4, Young's modulus E_1 of 7.2×10^{10} $\mathrm{N/m}^2$, density ρ_1 of 2700 $\mathrm{kg/m}^3$, area A_1 of 1.29×10^{-4} m^2, and length L_1 of 1 m. The following parameters are used for each vertical beam: width a_2 of 0.0508 m, thickness b_2 of 0.0127 m, moment of inertia I_2 of 8.67×10^{-12} m^4, Young's modulus E_2 of 1×10^9 $\mathrm{N/m}^2$, density ρ_2 of 1000 $\mathrm{kg/m}^3$, area A_2 of 6.45×10^{-5} m^2, and length L_2 of 3.0 m. Figure 2 is a plot of the transfer function of horizontal beam displacement divided by input force for an external force applied to the horizontal beam at $a = 0.8$ m. The solid line is the dynamic foundation model developed in equations (1)–(30) and the dot symbol is the discrete foundation model given by equations (38)–(40). The models are compared at a frequency of 11 Hz, a low value where the dynamic beam responses of the foundation approach the model using the constant spring values in equations (39) and (40). At these low frequencies, the result is that both models obtain the same values for the transfer function between 0 and 10 rad/m.

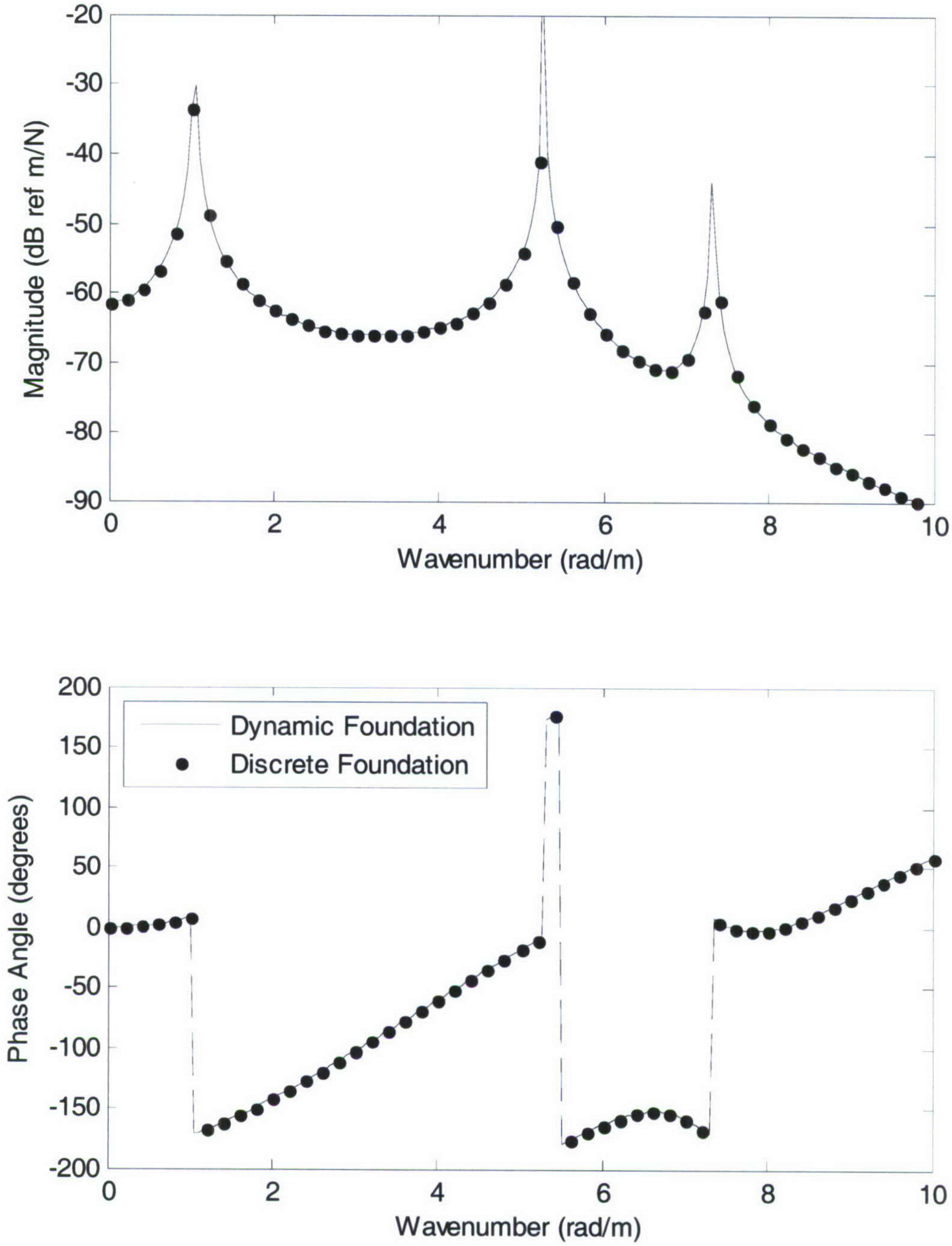

Figure 2. Comparison of Dynamic Foundation Model to Discrete Foundation Model

5. NUMERICAL EXAMPLE

A numerical example is now formulated with the three different loading cases derived in section 3. Using the parameters of the validation example (section 4), the model is now analyzed from a frequency range of 0 to 500 Hz, which is a range where the vertical beams behavior has to be modeled as a continuous medium to accurately represent the dynamics of the system. The first analysis is a comparison of system pole locations, which is not dependent on the forcing function. These are determined where

$$\det[\mathbf{A} + \mathbf{B} + \mathbf{C}] = 0 \tag{42}$$

is the wavenumber-frequency plane, and correspond to locations where the system's response goes to infinity. Figure 3 is a plot of the system poles determined using equation (42). The top plot is the system model with dynamic response of the vertical beams and was calculated using equations (19) and (30), and the bottom plot is the system model with discrete response of the vertical beams and was calculated using equations (38) through (40). Note that the traditional checkerboard pattern of the discrete model becomes more rounded using the dynamic model and that there are additional poles that appear in the dynamic model and correspond to dynamic behavior of the vertical beams.

The first loading case is that of a point force on the horizontal beam where the load vector is given by equation (30). Figure 4 is a plot of the magnitude of the horizontal beam displacement divided by a force F applied to the horizontal beam at $x = 0.8$ m. This response is shown in the wavenumber-frequency plane and the units are dB ref m/N. The top plot is the system model with dynamic response of the vertical beams and corresponds to equations (19) and (30), and the bottom plot is the system model with discrete response of the vertical beams and corresponds to equations (38) through (40). The second loading case is that of a point moment on the horizontal beam where the load vector is given by equation (32). Figure 5 is a plot of the magnitude of the horizontal beam displacement divided by a moment M applied to the horizontal beam at $x = 0.8$ m. This response is shown in the wavenumber-frequency plane and the units are dB ref N^{-1}. The top plot is the system model with dynamic response of the vertical beams and corresponds to equations (19) and (32), and the bottom plot is the system model with discrete response of the vertical beams and corresponds to equations (38) through (40). The third

loading case is that of an axial displacement on the vertical beam where the load vector is given by equation (35). Figure 6 is a plot of the magnitude of the horizontal beam displacement divided by the magnitude of the applied axial displacement V on the lower end of a single vertical beam located at $x = 0.0$ m. This response is shown in the wavenumber-frequency plane and the units are dB (dimensionless). The top plot is the system model with dynamic response of the vertical beams and corresponds to equations (19) and (35), and the bottom plot is the system model with discrete response of the vertical beams and corresponds to equations (38) through (41).

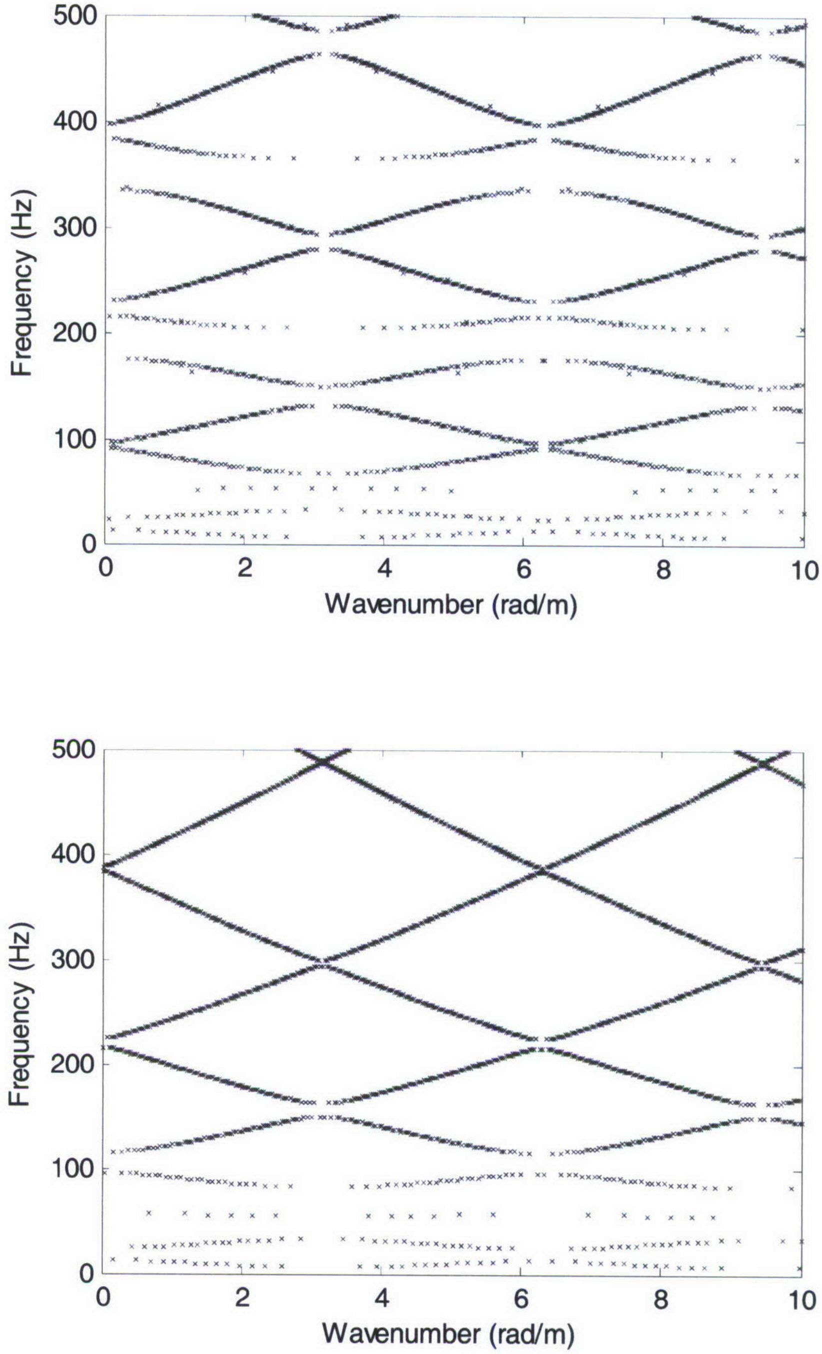

Figure 3. System Pole Locations in the Wavenumber-Frequency Plane (Results for Dynamic Model of the Vertical Beams (top) and Discrete Model of the Vertical Beams (bottom))

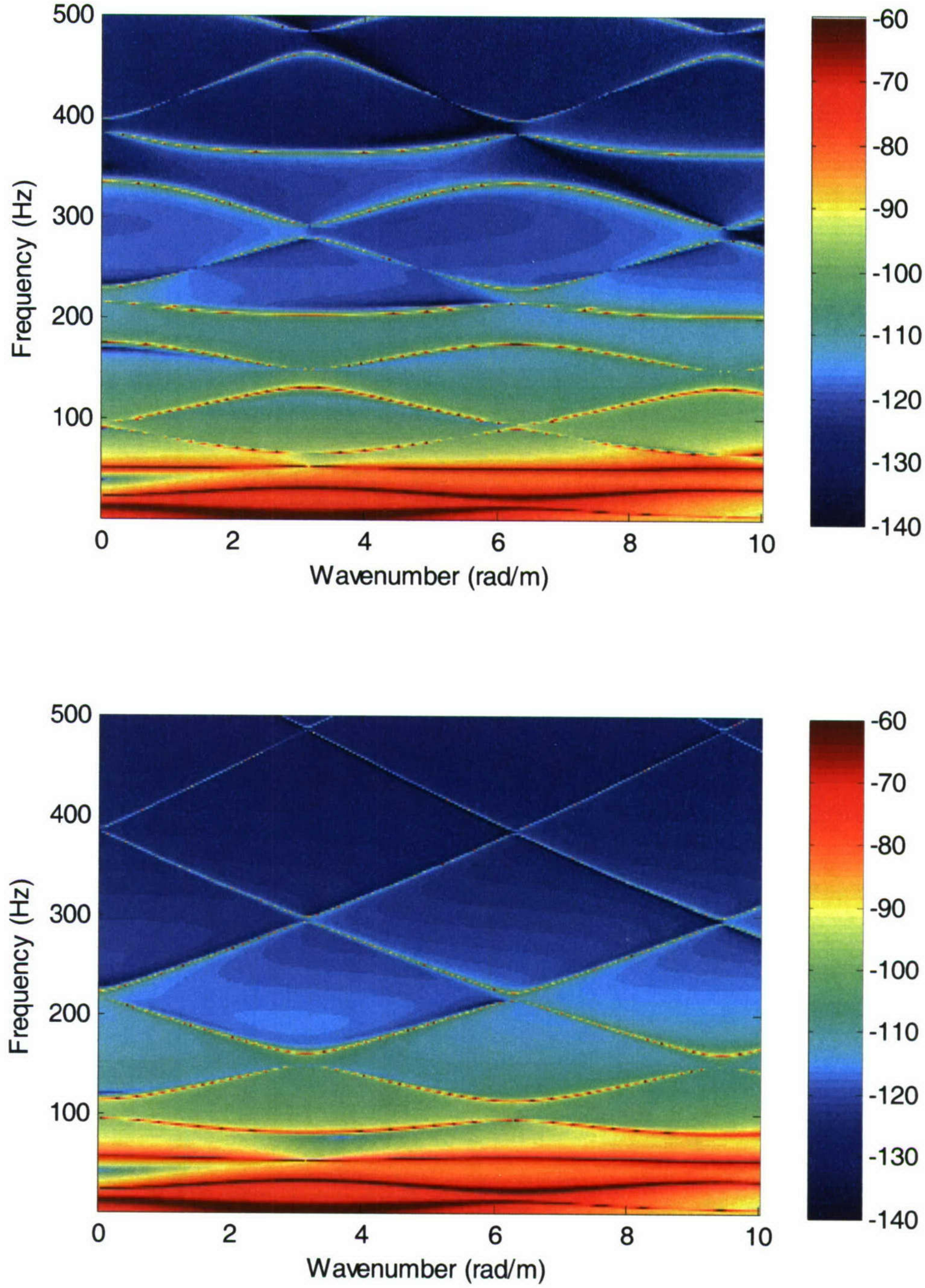

Figure 4. Magnitude of Horizontal Beam Displacement Divided by Input Force on Horizontal Beam (Results for Dynamic Model of the Vertical Beams (top) and Discrete Model of the Vertical Beams (bottom) (Units of dB ref m/N))

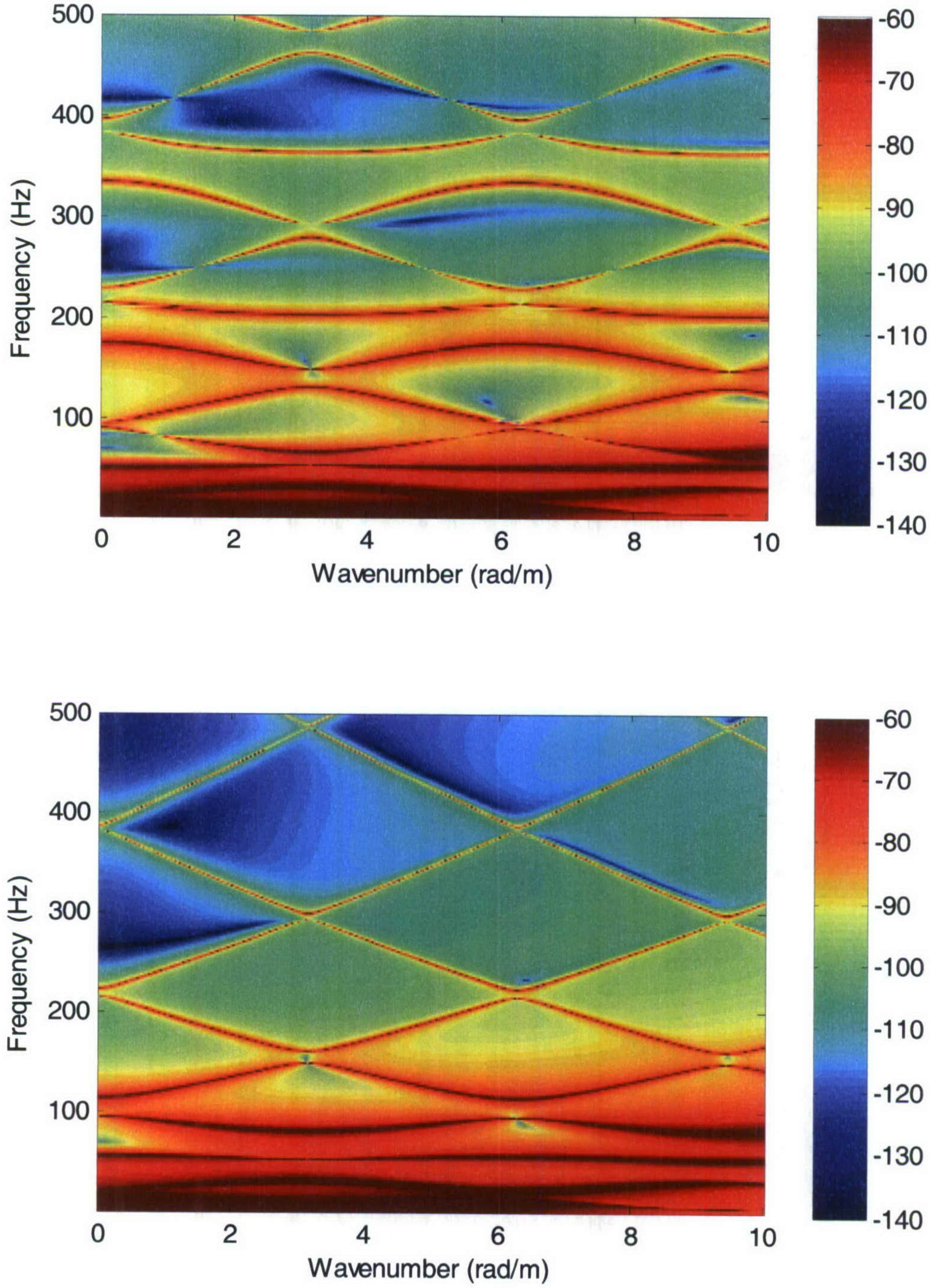

Figure 5. Magnitude of Horizontal Beam Displacement Divided by Input Moment on Horizontal Beam (Results for Dynamic Model of the Vertical Beams (top) and Discrete Model of the Vertical Beams (bottom) (Units of dB ref N^{-1}***))***

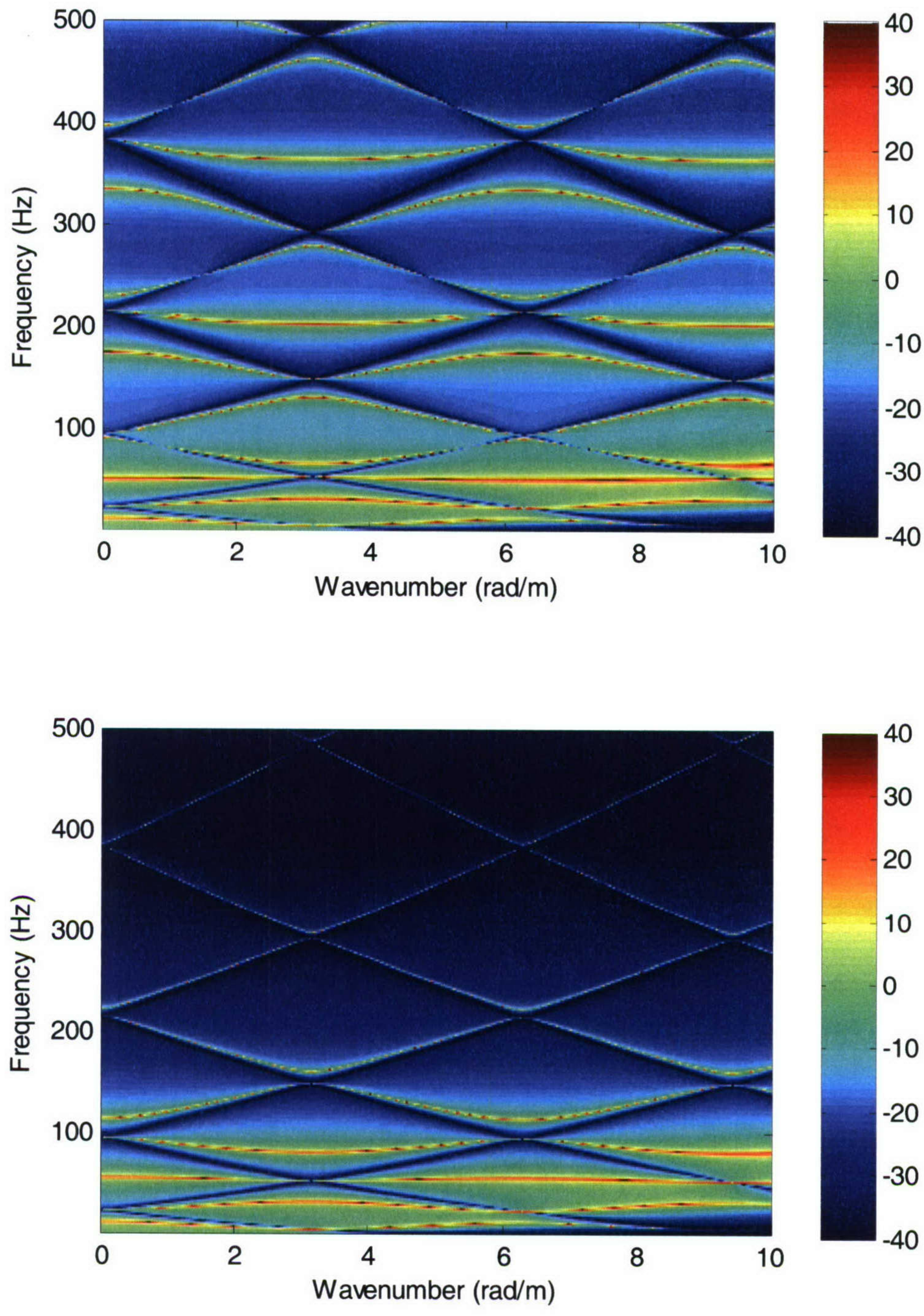

Figure 6. Magnitude of Horizontal Beam Displacement Divided by Axial Displacement of the Vertical Beam at x = 0 (Results for Dynamic Model of the Vertical Beam (top) and Discrete Model of the Vertical Beam (bottom) (Units of dB))

6. CONCLUSIONS

The equations of motion for a beam supported by a set of periodic support beams have been derived, and the displacements have been calculated in the wavenumber-frequency domain. This solution has been compared to a previously developed system where the beams were modeled as discrete springs, illustrating the effects of the dynamic response of the support beams. It was shown that at higher frequencies this response changes dramatically when the support models admit wave propagation.

7. REFERENCES

1. K. F. Graff, *Wave Motion in Elastic Solids*, Dover Publications, New York, 1975.

2. P. M. Belotserkovskiy, "Forced Oscillations and Resonances of Infinite Periodic Strings," *Journal of Sound and Vibration*, vol. 204, no. 1, 1997, pp. 41–57.

3. P. M. Belotserkovskiy, "Periodic String Response to an Impact and a Suddenly Applied Concentrated Stationary Force," *Journal of Sound and Vibration*, vol. 228, no. 1, 1999, pp. 51–68.

4. D. J. Mead and Y. Yaman, "The Response of Infinite Periodic Beams to Point Harmonic Forces: A Flexural Wave Analysis," *Journal of Sound and Vibration*, vol. 144, no. 3, 1991, pp. 507-530.

5. M. A. Heckl, "Coupled Waves on a Periodically Supported Timoshenko Beam," *Journal of Sound and Vibration*, vol. 252, no. 5, 2002, pp. 849-882.

6. D. J. Mead and N. S. Bardell, "Free Vibration of a Thin Cylindrical Shell with Periodic Circumferential Stiffeners," *Journal of Sound and Vibration*, vol. 115, no. 3, 1987, pp. 499-520.

7. R. C. Loftman and D. B. Bliss, "Scattering From Fluid-Loaded Cylindrical Shell With Periodic Circumferential Constraints Using Analytical/Numerical Matching," *Journal of the Acoustical Society of America*, vol. 106, no. 3, 1999, pp. 1271-1283.

8. B. R. Mace, "Periodically Stiffened Fluid-Loaded Plates, I: Response to Convected Harmonic Pressure and Free Wave Propagation," *Journal of Sound and Vibration*, vol. 73, no. 4, 1980, pp. 473-486.

9. B. R. Mace, "Periodically Stiffened Fluid-Loaded Plates, II: Response to Line and Point Forces," *Journal of Sound and Vibration*, vol. 73, no. 4, 1980, pp. 487-504.

10. G. P. Eatwell and D. Butler, "The Response of a Fluid-Loaded, Beam-Stiffened Plate," *Journal of Sound and Vibration*, vol. 84, no. 3, 1982, pp. 371-388.

11. A. J. Hull, "Dynamic Response of an Elastic Plate Containing Periodic Masses," *Journal of Sound and Vibration*, vol. 310, no. 1 and 2, 2008, pp. 1-20.

12. D. J. Mead and K. K. Pujara, "Space-Harmonic Analysis of Periodically Supported Beams: Response to Convected Random Loading," *Journal of Sound and Vibration*, vol. 14, no. 4, 1971, pp. 525-541.

INITIAL DISTRIBUTION LIST

Addressee	No. of Copies
Office of Naval Research (Code 333—D. Drumheller)	2
Defense Technical Information Center	2
Center for Naval Analyses	1